# Controlling quantum resonances in photonic crystals and thin films with electromagnetically induced transparency

C. H. Raymond Ooi[1,2,*] and C. H. Kam[3]
[1]*Department of Physics, University of Malaya, 50603 Kuala Lumpur, Malaysia*
[2]*School of Engineering, Monash University, Jalan Lagoon Selatan, Bandar Sunway, 46150 Selangor DarulEhsan, Malaysia*
[3]*School of Electrical & Electronic Engineering, Nanyang Technological University, Nanyang Avenue, 639798 Singapore, Singapore*
(Received 3 February 2010; revised manuscript received 12 April 2010; published 25 May 2010)

Quantum coherence or phaseonium medium with electromagnetic-induced transparency (EIT) may have been widely explored, but the incorporation of boundaries into finite structures like thin films and photonic crystals introduce additional resonant features. A narrow transmission peak exists in resonant medium due to multiple reflections and interference. The corresponding analytical formulas for absorptive and EIT media are derived. A double dip feature is found only for transverse magnetic polarized light, due to longitudinal electric field component in a Fabry-Perot thin film. We study these resonant features in a finite superlattice and discuss potential applications of the features. For phaseonium medium with laser-driven gain, transmission and reflection peaks beyond unity appear between the two EIT resonances. Realizations using solid-state materials such as doped crystals and quantum dots with potential applications are discussed.

DOI: 10.1103/PhysRevB.81.195119 PACS number(s): 42.50.Gy, 78.67.Pt, 42.50.Nn, 42.25.Bs

Electromagnetic-induced transparency (EIT)[1] is a quantum phenomena that has been widely studied in quantum and photonics systems, ranging from nonlinear optics[2] to metamaterials.[3] A medium becomes transparent to a probe field as the result of quantum interference when a laser field drives a transition in a three-level $\Lambda$ (Raman) scheme. Single resonance is split into double resonances, and its interference transforms an opaque medium into transparent. The same physics underlies the famous Fano resonance[4] in discrete-continuum quantum systems.

Classical interference can also occur in light as the result of multiple scattering/reflections off boundaries, such as artificially engineered structures. Superstructures composed of exotic materials, such as superconductors in photonic crystals, show new optical features.[5,6] We believe the combination of classical and quantum interference in a photonic crystal composed of dielectric and controllable quantum coherence medium can provide new interesting results. The effect of EIT in one-dimensional (1D) photonic crystal structure was first studied by Andre *et al.*[7] They created spatial periodic field grating by using counter-propagating control lasers, which forms periodic regions of high transparency (due to EIT) and high absorption corresponding to antinode and nodes of the control field, respectively.

In this paper, we consider similar structure but with different emphasis. We analyze the band structure of a superlattice composed alternating layers dielectric and quantum coherence (phaseonium)[8] medium driven by a laser field, as shown in Fig. 1. There are two types of resonances; (a) the usual Stark resonances—due to the ac Stark splitting of the quantum states as the result of the control laser and (b) structural resonances—due to the periodicity of the structure causes further splitting within each of the double resonances of the EIT. We will discuss the parameter that governs the size of the splitting. The physics of the former is well understood. However, the origin of the latter seems obscured despite its classical origin due to boundaries and this would be the main focus for analysis in the present work. The presence of boundaries in periodic structure also has interesting effects of the propagation of light.[6] We will discuss several useful applications of these effects.

## I. RESONANT AND PHASEONIUM MEDIA

The quantum coherence (phaseonium) medium is composed of three-level atoms where the control laser with Rabi frequency $\Omega_c$ gives electromagnetic induced transparency. The linear response is given by the dielectric function $\varepsilon_q(\omega)=\epsilon_b+\chi^{(1)}(\omega)$ with $\epsilon_b$ is the dielectric constant of the background medium and the field-dependent susceptibility[9]

$$\chi^{(1)}(\omega) \simeq i\frac{\mathcal{N}|\wp_{ab}|^2}{\hbar\varepsilon_o}\frac{[I_c w_{ac}/\Upsilon_{ac}^* - \Upsilon_{bc}^*(\omega)w_{ab}}{\Upsilon_{ab}(\omega)\Upsilon_{bc}^*(\omega)+I_c} \tag{1}$$

with $\Upsilon_{ac}=\gamma_{ac}-i\Delta_c$, $\Upsilon_{ab}(\omega)=\gamma_{ab}-i\Delta(\omega)$, and $\Upsilon_{bc}(\omega)=\gamma_{bc}-i[\Delta_c-\Delta(\omega)]$ and $w_{ab}=\rho_{aa}^{(0)}-\rho_{bb}^{(0)}$, $w_{ac}=\rho_{aa}^{(0)}-\rho_{cc}^{(0)}$. The effec-

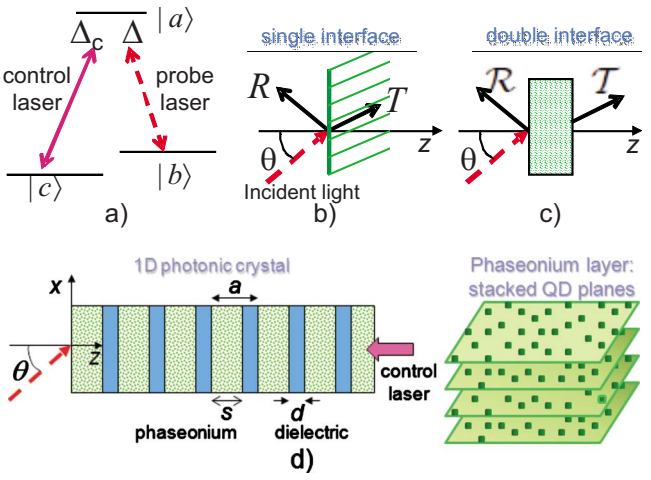


FIG. 1. (Color online) (a) Three levels scheme for phaseonium medium driven by a control laser with Rabi frequency $\Omega_c$. Schematics for: (a) single interface medium, (b) Fabry-Perot or thin film (double-interface) medium, and (d) superlattice composed of finite number of alternating phaseonium and dielectric layers. The phaseonium medium (layer) can be a crystal film doped with rare-earth ion, or multiple quantum dot (QD) planes stacked together.

 

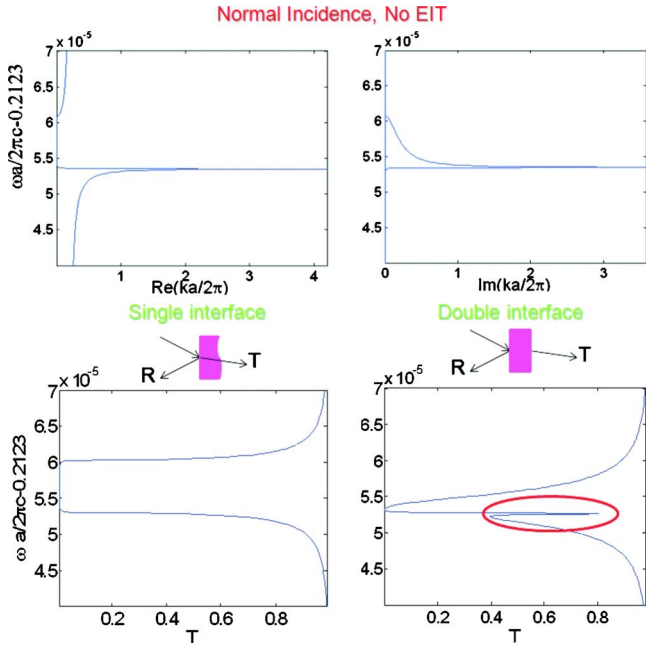


FIG. 2. (Color online) Reflection $R$ and transmission $T$ for resonance medium without EIT ($\Omega_c=0$) and normal incidence $\theta=0°$. The dielectric function is $\varepsilon_q(\omega,\Omega_c=0)$. For double interface, the thickness is $d=0.2$ $\mu$m. Both polarizations give identical results due to normal incidence. The narrow resonance is emphasized by a (red) circle. We use the following parameters for quantum dot based on Ref. 10: $\nu_c=\omega_{ac}=\omega_{ab}=10^{15}$ s$^{-1}$ ($\lambda\sim 2$ $\mu$m), $|\wp_{ab}|=8\times10^{-30}$ Cm, $\mathcal{N}=10^{24}$ m$^{-3}$, and $\gamma_{ac}=\gamma_{ab}=0.5\times10^{8}$ s$^{-1}$. For simplicity we use $\gamma_{bc}=0$, $\varepsilon_b=1$, and $\rho_{bb}^{(0)}=1$.

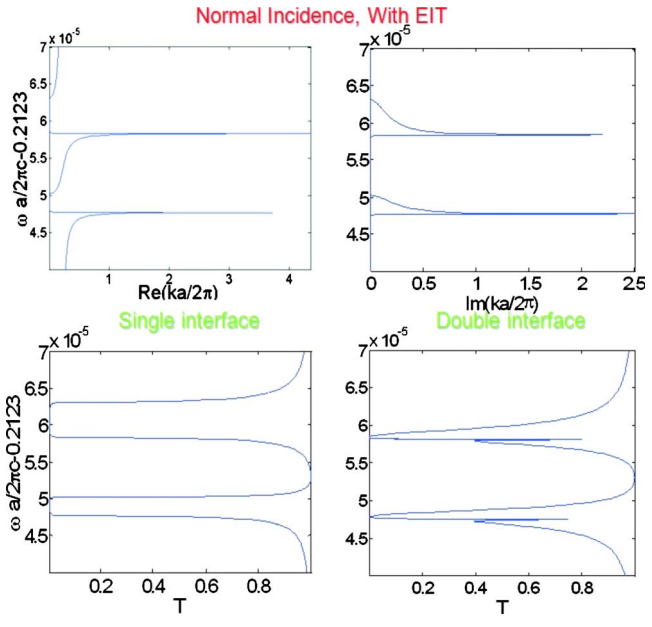


FIG. 3. (Color online) Reflection $R$ and transmission $T$ for resonance medium with EIT, $\Omega_c=500\gamma_{ac}$ and normal incidence $\theta=0°$. Other parameters are the same as in Fig. 2.

tive decoherences are $\gamma_{ac}=\frac{\Gamma_c+\Gamma_b}{2}+\gamma_{ac}^d$ and $\gamma_{ab}=\frac{\Gamma_c+\Gamma_b}{2}+\gamma_{ab}^d$ with $\Gamma_b$ and $\Gamma_c$ as the spontaneous emission rates, $\gamma_{ac}^d$ and $\gamma_{ab}^d$ are dephasing rates, $\Delta(\omega)=\omega-\omega_{ab}$ and $\Delta_c=\nu_c-\omega_{ac}$ are the detunings. The zeroth order populations[9] can be written as

$$\rho_{cc}^{(0)}=0.5-\xi,\quad \xi=I_c(\Gamma_b+\gamma_{bc})/2D, \tag{2}$$

$$\rho_{aa}^{(0)}=I_c\gamma_{bc}/D, \tag{3}$$

where $D=\gamma_{bc}(2\Gamma_b\Gamma_c+3I)+\Gamma_bI_c$ and $I_c=|\Omega_c|^2$. Atomic motion that gives Doppler broadening is not included since we are mainly concerned with nonmoving emitters in condensed materials. We plot the dispersion $\omega$ versus Re($k$) and Im($k$), $k=\omega\sqrt{\varepsilon_q(\omega)}/c$ for cases with and without EIT in Figs. 2 and 3. The incident probe field is sufficiently weak that the medium remains linear and nonlinear effects with double Raman transitions[11] are negligible. Note that Eq. (1) applies for lossy medium with single-absorption resonance by setting $\Omega_c=0$. The optics of this system is related to the recent Lenserf reflection.[12]

### A. $R$ and $T$ for single and double interfaces

Interference of waves from multiple reflections and refractions at boundaries can give rise to interesting resonant structures. In order to gain some physical understanding on this effect, let us now analyze the transmission and reflection for the simplest cases, medium with one and two interfaces. For single interface between incident medium $i$ and the quantum coherence medium $q$ we use the well-known Fresnel relations $r_{iq}^{(p)}=\frac{\varepsilon_qk_{iz}-\varepsilon_ik_{qz}}{\varepsilon_qk_{iz}+\varepsilon_ik_{qz}}$, $t_{iq}^{(p)}=\frac{2\sqrt{\varepsilon_q\varepsilon_i}k_{iz}}{\varepsilon_qk_{iz}+\varepsilon_ik_{qz}}$ and $r_{iq}^{(s)}=\frac{k_{iz}-k_{qz}}{k_{iz}+k_{qz}}$, $t_{iq}^{(s)}=\frac{2k_{iz}}{k_{iz}+k_{qz}}$ for (TM)$p$ and (TE)$s$ polarizations, respectively. For double interface, or Fabry-Perot etalon of thickness $d$ between input ($i$) and output ($o$) fields, $\tilde{r}_{io}=\frac{r_{iq}+r_{qo}f^2}{1+r_{iq}r_{qo}f^2}$, $\tilde{t}_{io}=\frac{t_{iq}t_{qo}f}{1+r_{iq}r_{qo}f^2}$, where $f=\exp(ik_{qz}d)$. The transmittance for single interface, $T=\frac{k_{iz}}{k_{qz}}|t_{iq}|^2$, and for double interface, $\mathcal{T}=|\tilde{t}_{io}|^2$, are computed in Figs. 2–5 for incident fields $\theta=0°$ and 45° for both polarizations. Similarly, the reflectance can be computed using $R=|r_{iq}|^2$, $\mathcal{R}=|\tilde{r}_{io}|^2$.

### B. $R$ and $T$ for superlattice

For superlattice with finite number of dielectric-phaseonium pairs, the band structure ($\omega$ versus $K$), reflection $R=|r^2|$, and transmission $T=|t^2|$ are computed in a standard way from the well-known[13] reflection and transmission coefficients

$$r=\frac{(M_{11}+M_{12}p_f)p_i-(M_{21}+M_{22}p_f)}{(M_{11}+M_{12}p_f)p_i+(M_{21}+M_{22}p_f)}, \tag{4}$$

$$t=\frac{s_{if}2p_i}{(M_{11}+M_{12}p_f)p_i+(M_{21}+M_{22}p_f)}, \tag{5}$$

where $M_{ij}$ are the components of the matrix

$$M=\begin{pmatrix} m'_{11}U_{N-1}-U_{N-2} & m'_{12}U_{N-1} \\ m'_{21}U_{N-1} & m'_{22}U_{N-1}-U_{N-2}\end{pmatrix}. \tag{6}$$

$m'_{ij}$ are components of $2\times2$ matrix $m'=(m_2m_1)^{-1}$,

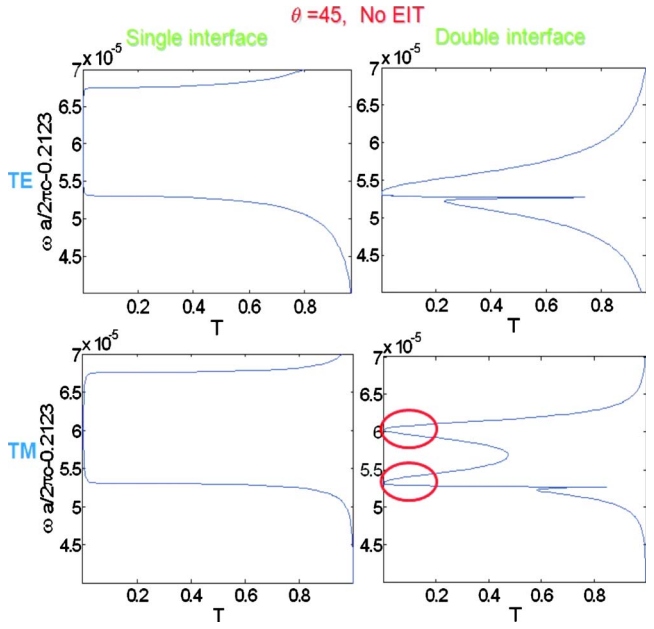


FIG. 4. (Color online) Reflection $R$ and transmission $T$ for resonance medium without EIT ($\Omega_c=0$) and $\theta=45°$. Other parameters are as in Fig. 2. Note that additional splitting occurs for $p$-polarized case even without EIT. Double dip feature is circled (in red).

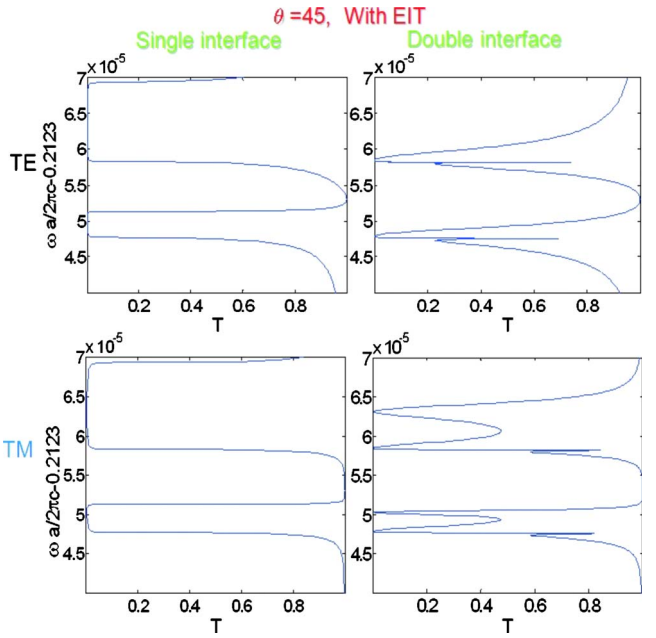


FIG. 5. (Color online) Reflection $R$ and transmission $T$ for resonance medium with EIT ($\Omega_c=500\gamma_{ac}$) and $\theta=45°$. Other parameters are as in Fig. 2. Four transmission dips (quadrupole resonances) can be seen when EIT is present.

$$m_j = \begin{pmatrix} \cos\beta_j & i\dfrac{\sin\beta_j}{p_j} \\ ip_j \sin\beta_j & \cos\beta_j \end{pmatrix}, \quad j = 1 \text{ or } 2,$$

$U_N=\frac{\sin(N+1)Ka}{\sin Ka}$, $\beta_1=k_{1z}d$, $\beta_2=k_{2z}s$, $k_{jz}=\frac{\omega}{c}\sqrt{\varepsilon_j-\varepsilon_i\sin^2\theta}$, and $N$ is the number of phaseonium-dielectric layers.

For TE-polarized light, $p_j=\zeta\sqrt{\varepsilon_j}\cos\theta_j=\zeta\frac{k_{jz}}{\omega c}$, $\zeta=\sqrt{\varepsilon_0/\mu_0}$, and $s_{if}=1$. For TM-polarized light, $p_j=k_{jz}/\zeta k_j\sqrt{\varepsilon_j}$ and $s_{if}=\sqrt{\varepsilon_i/\varepsilon_f}$, $i$ is the input/incident medium and $f$ is the final (output) medium. We use $\varepsilon_1=1$ and $\varepsilon_2=\varepsilon_q(\omega)$ for the resonant (absorptive or EIT) medium to obtain the results below.

## II. RESULTS

We analyze the optical effects of the finite structures with EIT medium by computing the dispersion of EIT; the reflection and transmission spectra for single interface, double interface, and superlattice; and the band structure.

### A. Narrow resonance and double dip

For normal incidence $\theta=0°$, the $p$ and $s$ polarizations give identical results (Figs. 2 and 3). In the absence of control field ($\Omega_c=0$ no EIT), a single (fine) *narrow resonance* peak emerges from the absorption window in transmission spectra for the case of double interface, i.e., a thin layer composed of lossy medium, as shown in Figs. 2 and 4. Note that this feature does not exist in bulk medium with constant dielectric. The width and location of the resonance depend on the thickness $d$ of the medium. The narrow feature is related to the recent work with array of absorbing nanoparticles.[14] This effect can be understood as the result of interference of the refracted wave and internally reflected waves from the two interfaces of the single slab, creating a cancellation of absorption within a narrow transmission window in the absence of EIT effect (normal absorbing medium). In other words, the narrow transmission peak (Fig. 2) corresponds to the so-called quasibound mode due to multiple interference of the absorption modes.

For the case of single-slab phaseonium, there are two mechanisms involved that create the resonant features. In the presence of EIT (phaseonium medium), however, the single resonance peak is split into double resonances (Fig. 4) by quantum interference (hole burning). Each resonance carries along the quasibounded mode, thus creating two narrow transmission peaks within the two absorption peaks.

In order to gain physical insight on the narrow feature, let us analyze the transmission for $s$-polarized light in normal incidence. Using $\tilde{t}_{io}$ expression above, we have

$$T=\frac{16|\varepsilon_q|}{|(1+\sqrt{\varepsilon_q})^2e^{-i\beta\sqrt{\varepsilon_q}}-(1-\sqrt{\varepsilon_q})^2e^{i\beta\sqrt{\varepsilon_q}}|^2}, \tag{7}$$

where $\beta=\omega d/c$. Equation (7) generally applies for any complex function of $\varepsilon_q$ and can be simplified to a more insightful form. In the absence of EIT, the dielectric function (without Doppler effect) is $\varepsilon_q(\omega)=1-\frac{\eta}{i\Gamma_b/2+\Delta}$ with $\eta=\frac{\mathcal{N}|\wp_{ab}|^2}{\hbar\varepsilon_o}$, corresponds to an absorptive medium with single resonance. By neglecting the $\Gamma_b/2$, the dielectric function is real $\varepsilon_q(\omega)\simeq 1-\frac{\eta}{\Delta}=\epsilon(\Delta)$, which leads to a more suggestive expression

$$T_{\text{abs}}\simeq\frac{16\epsilon}{(1+\sqrt{\epsilon})^4+(1-\sqrt{\epsilon})^4-\left(\dfrac{\eta}{\Delta}\right)^2 2\cos(\beta\sqrt{\epsilon})}. \tag{8}$$

At around the resonance, $\frac{\eta}{\Delta}(\gg 1)$ is large and $\sqrt{\epsilon}\simeq i\sqrt{\frac{\eta}{\Delta}}$, giving a simple expression

$$T_{\text{abs}} \simeq \frac{8}{\frac{\eta}{\Delta}\left[\cosh\left(\beta\sqrt{\frac{\eta}{\Delta}}\right)-1\right]+6}, \tag{9}$$

which contains hyperbolic function in the denominator, containing a pole that is partly responsible for the narrow transmission peak within a broader resonant dip, as in Fig. 2. The "1" and "6" in the denominator of Eq. (9) are necessary to avoid singularity in the profile despite the condition $\frac{\eta}{\Delta} \gg 1$.

For the case with EIT we obtain an analytical expression, in the same way, simply replacing $\sqrt{\frac{\eta}{\Delta}}$ by $\sqrt{\frac{\eta(\Delta_c-\Delta)}{\Delta(\Delta_c-\Delta)+I_c}}$, giving

$$T_{\text{EIT}} \simeq \frac{8}{\frac{\eta(\Delta_c-\Delta)}{\Delta(\Delta_c-\Delta)+I_c}\left(\cosh\beta\sqrt{\frac{\eta(\Delta_c-\Delta)}{\Delta(\Delta_c-\Delta)+I_c}}-1\right)+6}, \tag{10}$$

where $\Delta(\Delta_c-\Delta)+I_c$ gives the double resonances at $\Delta^{\pm} = \frac{1}{2}(\Delta_c \pm \sqrt{\Delta_c^2+4I_c})$.

Equations (8) and (10) are simple analytical expressions that correctly describe all the main features for double interface (from exact simulation) in Figs. 2 and 3, respectively. The presence of EIT splits the absorption peak into two and duplicates the narrow structure into two sets (Fig. 3). The doubling of the resonances is due to the splitting of the atomic levels by the control field. Here, we find that the two narrow resonance peaks provide *very precise* measurement of the width of the Autler-Townes splitting,[15] i.e., $2\Omega_c$.

In the case of $\theta$=45°, the *p*-polarized light gives an additional feature not found in the *s*-polarized light, i.e., a dip in the reflection peak and a peak in the transmission dip, creating *double dip* structures, Fig. 4. The spacing between the dips is found to be proportional to the medium number density $\mathcal{N}$. This feature could be used for measurement of the *optical density* of the phaseonium medium, and physical quantities like pressure and temperature that vary with the density of the medium. The EIT duplicates the narrow resonance and double dip features into two sets (Fig. 5), as in the case $\theta$=0°.

### B. Optical structures in superlattice

We now analyze the band structure, reflectance, and transmittance for superlattice with finite length. Figure 6(a) shows the results for zero control field, i.e., no EIT effect. It is interesting to note the double dip feature remains, but is shaped into more well-defined regions of absolute reflection or zero transmission. This is the result of multiple interference of the longitudinal component of electric field in the periodic structure. Figure 6(a) highlights [in (red) circle] the narrow transmission resonance, which remains exactly at 5.25, as in the case of double interface of Figs. 2 and 4.

In the presence of EIT (finite control laser field), Fig. 6(b) shows the two pairs of double dip are separated apart by $2\Omega_c$ (for $\gamma_{bc}$=0). The pairs are referred to as upper resonances (URs) and lower resonances (LRs). The double dip and narrow transmission features are also present, as in the case of double interface of Figs. 3 and 5. The plot for $R+T$ shows

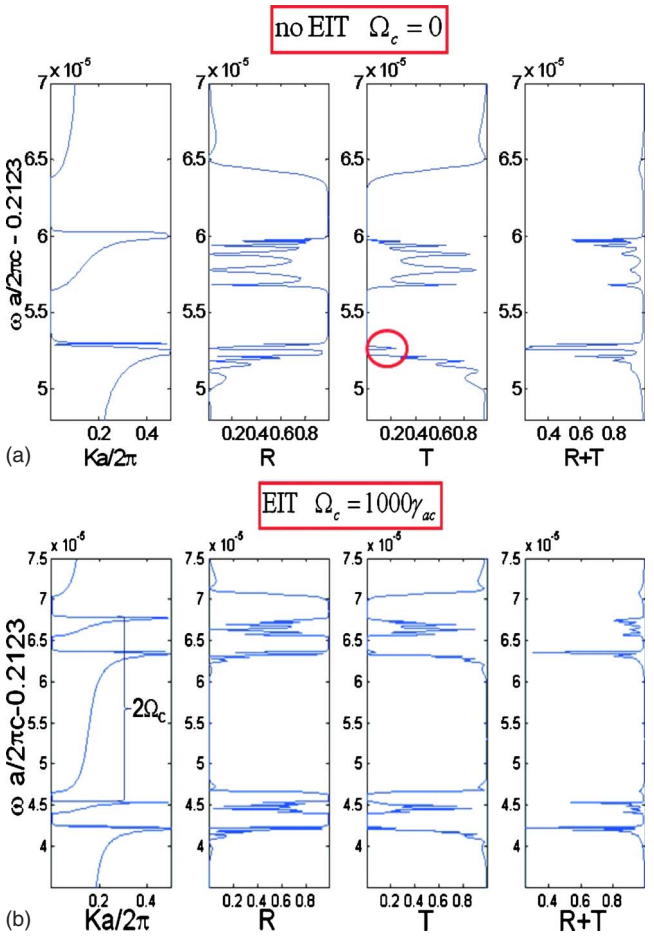


FIG. 6. (Color online) Band structure, reflection $R$, transmission $T$, and $R+T$ with TM-polarized light and $\theta$=45° for cases: (a) $\Omega_c$=0 (no EIT) and (b) $\Omega_c$=1000$\gamma_{ac}$. The superlattice parameters are $\varepsilon_d$=1, $a$=0.4 $\mu$m, $d$=0.5$a$, and $n$=8 layers. The transition parameters are the same as in Fig. 2. Band structure with four branches (corresponding to quadrupole resonances) can be seen when EIT is present. The (red) circle highlights the narrow resonance at around 5.25 in (a).

that the lossy regions always correspond to the transmission band between the double dip as well as the narrow transmission peak.

So, what are the effects resulting from the 1D photonic (phaseonium) crystal? The periodicity of the photonic crystal gives rise to well-defined band gaps as well as intricate features of the reflection/transmission spectra shown in Fig. 6. It provides extra degrees of freedom for controlling the spectra through the number of paired layers $N$ and the relative thickness of the dielectric layer $d/a$. Figure 7 shows how the widths of the two resonances [in (red) circles] within the UR and LR can be tuned by changing $d/a$. When the phaseonium layer is dominant, $d$=0.1$a$, Fig. 7(a), the dispersive branches become quite flat (slow group velocity, i.e., small $d\omega/dK$). The small relative thickness of the dielectric layer gives rise to wider double dip which corresponds to two narrow transmission peaks. On the other hand, if the structure is dominated by dielectric, i.e., thin phaseonium layer, $d$=0.9$a$=40 nm we obtain [Fig. 7(b)] two pairs of narrow

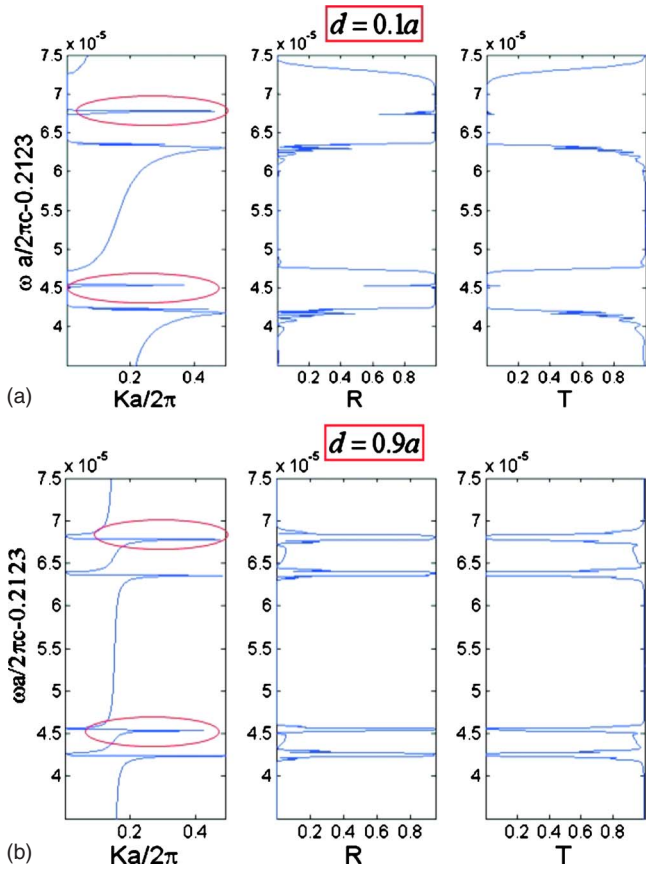


FIG. 7. (Color online) Band structures with TM polarization and $\theta=45°$ for different dielectric layer thickness $d$ show the variation in the structure resonances, (a) $d=0.1a$ and (b) $d=0.9a$. Here, $\Omega_c=1000\gamma_{ac}$. Other parameters are as in Fig. 6.

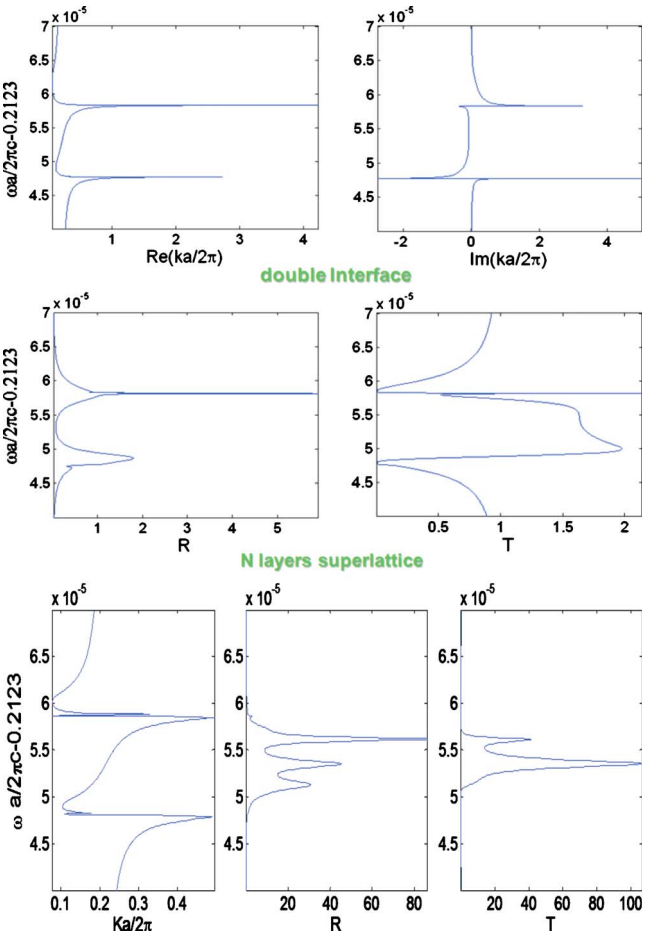


FIG. 8. (Color online) Dispersions, reflection ($R$), and transmission ($T$) for EIT medium with small populations in levels $c$ and $a$, $\rho_{cc}^{(0)}=0.002$, $\rho_{aa}^{(0)}=0.001$, and $\theta=0°$. Note that $R$ and $T$ are beyond unity for thin-film case and superlattice. Here, $\Omega_c=500\gamma_{ac}$. Other parameters are as in Fig. 6. Unlike the above figures, here, the two parameters are finite, $\rho_{aa}^{(0)}\neq 0$, $\gamma_{bc}\neq 0$. We set $\rho_{cc}^{(0)}=0.002$ and obtain $\rho_{aa}^{(0)}=I_c\gamma_{bc}/D$ consistently by solving $\gamma_{bc}$ in $I(\Gamma_b+\gamma_{bc})/2D=\xi=1/2-\rho_{cc}^{(0)}$.

reflection peaks corresponding to two pairs of narrow dips (with two broader transmission bands).

If initially there is population in level $c$, the first term in Eq. (1) contributes to the imaginary part of the susceptibility. Thus $w_{ac}<0$ is expected to yield large gain since in gainless situation, Im $\chi^{(1)}>0$. Figure 8 shows the case where levels $c$ and $a$ have small populations $\rho_{cc}^{(0)}=0.002$ [$\rho_{aa}^{(0)}=0.001$ based on Eqs. (2) and (3)] giving an inversionless gain[16] proportional to $\rho_{cc}^{(0)}I_c$, based on the negative imaginary part of $\chi^{(1)}$ in Eq. (1). For single interface, $R$ and $T$ do not exceed unity. Only for the double interface and superlattice, $R$ and $T$ can exceed unity since the probe field amplifies by acquiring extra energy from the control field. The "superunity" reflection peaks appear around the two EIT resonances while the plateau of the transmission spectra lies between the resonances. For superlattice, it is interesting that the superunity peaks of both $R$ and $T$ are between the two EIT resonances, i.e., the region of transparency and gain.

Figure 9 shows the variations in $R$ and $T$ spectra with $\rho_{cc}^{(0)}$ for the superlattice, for different decay rate, densities and driving fields. For smaller control field, i.e., $\Omega_c=50\gamma_{ac}$, a series of high (twin) peaks can be seen as $\rho_{cc}^{(0)}$ increases toward $\rho_{cc,\max}^{(0)}$. However, such high transmission and reflection peaks do not appear for values beyond $\rho_{cc,\max}^{(0)}$. For $\mathcal{N}=10^{23}$ m$^{-3}$ with $|\wp_{ab}|=8\times10^{-30}$ Cm the maximum peak is at $\rho_{cc,\max}^{(0)}\simeq 0.024$ [Figs. 9(a) and 9(b)]. When the density increases by ten times to $\mathcal{N}=10^{24}$ m$^{-3}$, the peak location decreases by ten times. However, in Fig. 9(c), the $\gamma_{ac}$ is increased by two times, which explains why the peak is at $\rho_{cc,\max}^{(0)}\simeq 0.0048$ instead of 0.0024. Analysis of Fig. 9 leads to an empirical scaling formula which relates the new parameters (with "prime") with the old ones,

$$\rho_{cc,\max}^{(0)\prime}/\rho_{cc,\max}^{(0)}=\frac{\mathcal{N}}{\mathcal{N}'}\frac{\gamma_{ac}'}{\gamma_{ac}}. \tag{11}$$

## III. PRACTICAL ASPECTS

We elaborate on the feasibility of using solid-state materials as the phaseonium medium and discuss potential applications of the spectral features found above.

### A. Solid-state implementations

Although the EIT model presented is based on atomic systems, it is applicable to solid-state materials. The phaseo-

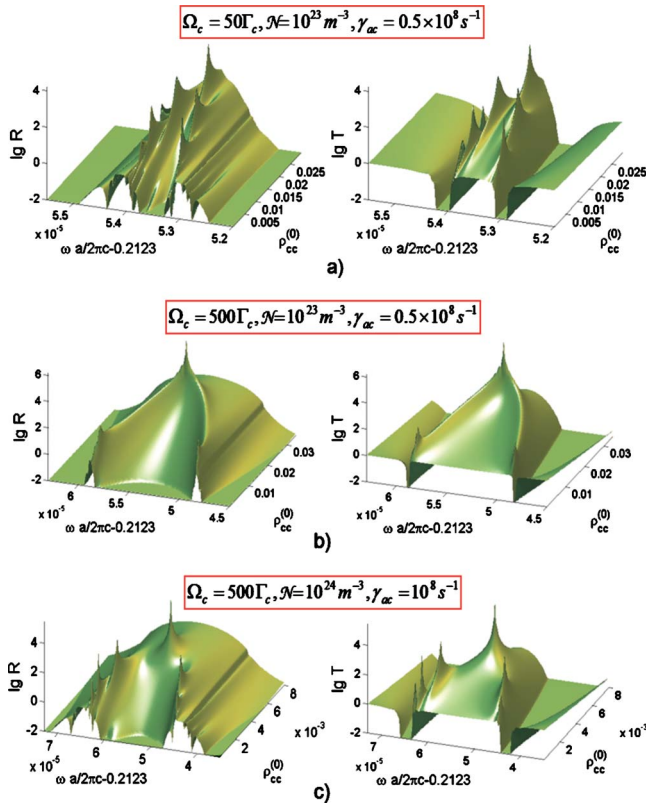


FIG. 9. (Color online) Reflection ($R$) and transmission ($T$) spectra (in log10 scale) versus $\rho_{cc}(0)$ for superlattice with EIT medium for different control Rabi frequency $\Omega_c$, number density $\mathcal{N}$, and decay rates $\Gamma_c$ for $|\wp_{ab}|=8\times10^{-30}$ Cm. The highest peaks in (a), (b), and (c) occur at around $\rho_{cc,\max}^{(0)}=0.024$, 0.024, and 0.0048, respectively, where the twin peaks converge to a single peak. Other parameters are the same as in Fig. 8. For each $\rho_{cc}^{(0)}$ we obtain $\rho_{aa}^{(0)}$ consistently after solving for $\gamma_{bc}$ using $I_c(\Gamma_b+\gamma_{bc})/2D=1/2-\rho_{cc}^{(0)}$.

nium medium/layer can be a crystal doped with rare-earth (lanthanide) elements or a dielectric matrix embedded with quantum dots. In the doped crystal case, the dephasing rates can be made close to those in atomic gas,[17] and the small decoherence between the ground hyperfine levels, i.e., around 20 kHz for $Pr^{3+}$: $La_2(WO_4)_3$,[18] despite phonon broadening, by matching the radii of the dopant and host atoms as well as through cooling down to 2 K. Thus, the parameters used in the above Figs. 2–9 are applicable to doped crystal case.

For quantum dots distributed in a dielectric matrix, the three-level $\Lambda$ scheme is formed through the transitions between two exciton states $|\pm\rangle$ and a biexciton (excited) state $X_2$.[19] Based on Ref. 10, the energy separations are typically between infrared and optical regimes, i.e., $\omega_{ac}\simeq\omega_{ab}\simeq10^{15}$ s$^{-1}$($\lambda\simeq2$ $\mu$m). The dipole moment is about 50 times larger than atomic case, i.e., $|\wp_{ab}|=3\times10^{-28}$ Cm. The number density for a single quantum dot is $\mathcal{N}_1=2\times10^{23}$ m$^{-3}$, obtained from $\mathcal{N}_1=\hbar\Gamma/V=(5000\ \text{nm}^3)^{-1}$ ($\Gamma$ is the confinement factor, $V=9\times10^{-25}$ m$^3$ is the dot volume). For multiple quantum dots produced by *atomic-layer epitaxy*, the typical area density is $\eta=3\times10^{14}$ m$^{-2}$ and below. By choosing the distance between the layers to be $\delta=76$ nm ($\gtrsim2/\sqrt{\pi\eta}=64$ nm), we have the effective number density $\mathcal{N}=\eta\mathcal{N}_1V/\delta\simeq7.11\times10^{20}$ m$^{-3}$, which gives a value for the product $|\wp_{ab}|^2\mathcal{N}$ [$\propto\chi^{(1)}$ in Eq. (1)] that is almost the same as that obtained using the parameters for atomic gases, i.e., $|\wp_{ab}|=8\times10^{-30}$ Cm, $\mathcal{N}=10^{24}$ m$^{-3}$. However, the decoherence rates for the quantum dots at temperature of a few Kelvin is tenfold larger (i.e., $\gamma_{ac}=\gamma_{ab}=5\times10^9$ s$^{-1}$) than atomic rates, due to the large dephasings. We find that this only causes the separation between the two sets of peaks [more clearly seen in Fig. 9(b)] to increase by ten times (figure not shown), while the main features of the spectra (such as $\rho_{cc,\max}^{(0)}$) remain unaffected. The features in Fig. 9 satisfy the scaling laws discussed above, showing the applicability of the $\Lambda$ scheme to stacked layers of quantum dots.

Thus, the above results that were computed using atomic $\Lambda$ scheme parameters are applicable to phaseonium medium constructed from doped crystal and stacked layers of quantum dots.

### B. Potential applications

The results can provide new applications. For example, the transmission peak is much narrower than the EIT width and therefore could be useful in high-precision spectroscopy as well as ultraslow light buffer or optical memory in all-photonic circuits. Also, the narrow peaks in Fig. 7(b) could be used to construct *correlated band-edge laser* since the two peaks are strongly correlated due to EIT. In the case of finite gain in the multilayer case, the narrow peak with high transmission could be used as a gain medium to construct a laser with ultranarrow linewidth. The presence of gain in active structures can be used to compensate for absorption loss, promoting the practical use of metamaterials and photonic crystals to a wider domain. Since the location of the narrow peak depends on the thickness of the phaseonium layer, it could be useful as a sensitive piezo-optic switch.

## IV. CONCLUSIONS

We have studied the effects of structural boundaries on quantum resonances. We found useful narrow resonant feature in the transmission and reflection spectra of thin film and superlattice composed of absorbing or quantum coherence (phaseonium) medium. The narrow feature is due to the combination of material resonance and bounded mode present within a thin slab; but does not occur either in bulk medium nor frequency region of dielectric function without resonance. We also study the spectra when the medium has gain. The features are supported by physical explanation and analytical formulas. These features can be engineered using solid-state materials such as doped crystal or quantum dots for developing functional photonic devices that can be controlled by the laser field and structural variables.

## ACKNOWLEDGMENTS

R.O. gratefully acknowledges Nanyang Technological University for hospitality during the recent research visit and Monash University for supporting the computational facility. This work is also supported by University of Malaya Research Grant RG111.

*bokooi73@yahoo.com; rooi@um.edu.my

[1] K. J. Boller, A. Imamoglu, and S. E. Harris, Phys. Rev. Lett. **66**, 2593 (1991); M. O. Scully and M. S. Zubairy, *Quantum Optics* (Cambridge University Press, Cambridge, England, 1997).
[2] S. E. Harris, J. E. Field, and A. Imamoglu, Phys. Rev. Lett. **64**, 1107 (1990).
[3] S. Zhang, D. A. Genov, Y. Wang, M. Liu, and X. Zhang, Phys. Rev. Lett. **101**, 047401 (2008).
[4] U. Fano, Phys. Rev. **124**, 1866 (1961).
[5] C. H. Raymond Ooi, T. C. Au Yeung, C. H. Kam, and T. K. Lim, Phys. Rev. B **61**, 5920 (2000).
[6] C. H. Raymond Ooi and C. H. Kam, J. Opt. Soc. Am. B **27**, 458 (2010).
[7] A. André, M. Bajcsy, A. S. Zibrov, and M. D. Lukin, Phys. Rev. Lett. **94**, 063902 (2005); M. Bajcsy, A. S. Zibrov, and M. D. Lukin, Nature (London) **426**, 638 (2003).
[8] M. O. Scully, Phys. Rep. **219**, 191 (1992).
[9] A. Javan, O. Kocharovskaya, H. Lee, and M. O. Scully, Phys. Rev. A **66**, 013805 (2002).
[10] C. J. Chang-Hasnain, P. C. Ku, J. Kim, and S. L. Chuang, Proc. IEEE **91**, 1884 (2003); D. Barettin, J. Houmark, B. Lassen, M. Willatzen, T. R. Nielsen, J. Mork, and A. P. Jauho, Phys. Rev. B **80**, 235304 (2009).
[11] Y. V. Rostovtsev, A. B. Matsko, and M. O. Scully, Phys. Rev. A **57**, 4919 (1998).
[12] A. Siegman, Opt. Photonics News **21**, 38 (2010).
[13] M. Born and E. Wolf, *Principles of Optics*, 7th ed. (Cambridge University Press, United Kingdom, 1999).
[14] V. Yannopapas, E. Paspalakis, and N. V. Vitanov, Phys. Rev. B **80**, 035104 (2009); G. Gantzounis, N. Stefanou, and V. Yannopapas, J. Phys.: Condens. Matter **17**, 1791 (2005).
[15] S. H. Autler and C. H. Townes, Phys. Rev. **100**, 703 (1955).
[16] S. E. Harris, Phys. Rev. Lett. **62**, 1033 (1989).
[17] R. Lauro, T. Chanelière, and J.-L. Le Gouët, Phys. Rev. A **79**, 053801 (2009).
[18] Ph. Goldner, O. Guillot-Noël, F. Beaudoux, Y. Le Du, J. Lejay, T. Chanelière, J.-L. Le Gouët, L. Rippe, A. Amari, A. Walther, and S. Kröll, Phys. Rev. A **79**, 033809 (2009).
[19] D. Gammon and D. G. Steel, Phys. Today **55** (10), 36 (2002).